



Published in final edited form as:

*Pain*. 2010 May ; 149(2): 284–295. doi:10.1016/j.pain.2010.02.022.

## Eccentric Muscle Contraction and Stretching Evoke Mechanical Hyperalgesia and Modulate CGRP and P2X<sub>3</sub> Expression in a Functionally Relevant Manner

Dean Dessem<sup>a,b</sup>, Ranjinidevi Ambalavanar<sup>a</sup>, Melena Evancho<sup>a</sup>, Aicha Moutanni<sup>a</sup>, Chandrasekhar Yallampalli<sup>c</sup>, and Guang Bai<sup>a,b</sup>

<sup>a</sup> Department of Neural and Pain Sciences, University of Maryland, 650 West Baltimore Street, Baltimore, MD 21201

<sup>b</sup> Graduate Program in Neuroscience, University of Maryland, Baltimore, MD

<sup>c</sup> Department of Obstetrics and Gynecology, University of Texas, Galveston, TX 77555

### Abstract

Non-invasive, movement-based models were used to investigate muscle pain. In rats, the masseter muscle was rapidly stretched or electrically stimulated during forced lengthening to produce eccentric muscle contractions (EC). Both EC and stretching disrupted scattered myofibers and produced intramuscular plasma extravasation. Pro-inflammatory cytokines (IL-1 $\beta$ , TNF- $\alpha$ , IL-6) and vascular endothelial growth factor (VEGF) were elevated in the masseter 24h following EC. At 48h, neutrophils increased and ED1 macrophages infiltrated myofibers while ED2 macrophages were abundant at 4d. Mechanical hyperalgesia was evident in the ipsilateral head 4h-4d after a single bout of EC and for 7d following multiple bouts (1 bout/d for 4d). Calcitonin gene-related peptide (CGRP) mRNA increased in the trigeminal ganglion 24h following EC while immunoreactive CGRP decreased. By 2d, CGRP-muscle afferent numbers equaled naive numbers implying that CGRP is released following EC and replenished within 2d. EC elevated P2X<sub>3</sub> mRNA and increased P2X<sub>3</sub>-muscle afferent neuron number for 12d while electrical stimulation without muscle contraction altered neither CGRP nor P2X<sub>3</sub> mRNA levels. Muscle stretching produced hyperalgesia for 2d whereas contraction alone produced no hyperalgesia. Stretching increased CGRP mRNA at 24h but not CGRP-muscle afferent number at 2–12d. In contrast, stretching significantly increased the number of P2X<sub>3</sub>-muscle afferent neurons for 12d. The sustained, elevated P2X<sub>3</sub> expression evoked by EC and stretching may enhance nociceptor responsiveness to ATP released during subsequent myofiber damage. Movement-based actions such as EC and muscle stretching produce unique tissue responses and modulate neuropeptide and nociceptive receptor expression in a manner particularly relevant to repeated muscle damage.

### Keywords

pain; muscle pain; delayed onset muscle soreness

---

Correspondence: Dean Dessem, Ph.D., Department of Neural and Pain Sciences, University of Maryland, 650 West Baltimore Street, Baltimore, MD 21201, Tel 410-706-7257, FAX 410-706-0193, ddessem@umaryland.edu.

**Publisher's Disclaimer:** This is a PDF file of an unedited manuscript that has been accepted for publication. As a service to our customers we are providing this early version of the manuscript. The manuscript will undergo copyediting, typesetting, and review of the resulting proof before it is published in its final citable form. Please note that during the production process errors may be discovered which could affect the content, and all legal disclaimers that apply to the journal pertain.

## 1. Introduction

Musculoskeletal pain is one of the most frequent symptoms encountered by primary care providers [48,57]. In spite of this prevalence, the mechanisms involved in deep tissue pain are poorly understood and current therapies are not only ineffective but can be dangerous [21,37,69]. Musculoskeletal disorders in the craniofacial region include temporomandibular disorders which frequently involve pain in the muscles of mastication [18,62]. Fibromyalgia, a musculoskeletal disorder characterized by widespread muscle pain, also frequently involves pain in craniofacial muscles [40,76,77].

There are no widely accepted models of muscle pain in part because previous models are invasive and do not reproduce the characteristics of muscle pain. A common experimental method used to study muscle pain is to inject complete Freund's adjuvant (CFA) into muscle [3,5,6,8,16,39,86]. Other exogenous substances (hypertonic saline, mustard oil, carrageenan, capsaicin) and endogenous (serotonin, bradykinin, ATP, TNF- $\alpha$ , NGF) substances have also been used to model muscle pain [26,29,42,49,<sup>63,78</sup>,87,88,94,98]. While these methods may provide insight into certain aspects of muscle pain such as pain produced by infection, poisoning and autoimmune dysfunction they do not incorporate movement or contractility, fundamental properties of muscle. For this reason we employed *in vivo* muscle contraction and rapid muscle stretching to study muscle nociceptive mechanisms.

Considerable evidence implicates the neuropeptide calcitonin gene-related peptide (CGRP) in deep tissue nociceptive mechanisms [14,80]. Recently there has been a resurgence of interest in the role of neuropeptides in pain, in part due to the development of neuropeptide antagonists which show considerable promise for the treatment of migraine headache [41,71]. We suspect that these neuropeptide antagonists may have broader therapeutic applications including muscle pain. Therefore we investigated the effects of muscle contraction and stretching on CGRP expression. We also examined P2X<sub>3</sub> receptor expression since trigeminal ganglion muscle afferent neurons express a high percentage of P2X<sub>3</sub> receptors [3] which can not only be upregulated by CGRP [28] but also potentially activated by ATP released from damaged or undamaged myofibers.

We investigated muscle pain in the masticatory muscles for several reasons. Not only is muscle tension commonly associated with temporomandibular disorders and craniofacial pain [36], but the masseter muscle also exhibits a reduced ability to repair following injury [73] and an increased tendency to undergo apoptosis [27]. Thus muscle damage, subsequent inflammation and increased primary afferent drive could initiate or exacerbate chronic craniofacial pain. A high percentage of craniofacial deep tissue primary afferent neurons also express the P2X<sub>3</sub> receptor and co-localize CGRP with P2X<sub>3</sub> [2].

We employed eccentric muscle contraction (EC) and rapid muscle stretching, movement-based stimuli, to produce muscle pain and inflammation. We characterize the EC and muscle stretching models by quantifying their effects on myofiber integrity, plasma extravasation, inflammatory cytokine levels and inflammatory cell density. We then examined the effects of EC and stretching on nocifensive behavior and the expression of neuropeptides and P2X receptors in the trigeminal ganglion thus providing unique insight into the mechanisms of muscle nociception by utilizing movement-based models.

## 2. Methods

Male Sprague Dawley rats (239–441g, n=198) were used for all experiments. Animals received humane care in compliance with the *Guide for the Care and Use of Laboratory Animals* (NIH publication no. 86-23, revised 1985) and the Use Committee and the Committee for Research and Ethical Issues of the IASP. All laboratory procedures were

reviewed and approved by the University of Maryland Animal Care and Use Committee. Every effort was made to minimize any suffering.

### 2.1. Eccentric muscle contraction and rapid muscle stretching

The skin overlying the masseter muscle was anesthetized by applying an anesthetic cream (2.5% lidocaine, 2.5% prilocaine). Two hours later, rats were anesthetized with isoflurane. A rod coupled to a stepping motor, torque transducer and potentiometer was then positioned in the diastema of the mandible. To produce eccentric muscle contractions, the masseter muscle was stimulated with 1s trains (100Hz, 0.3ms pulse) at 0.3Hz using custom-made surface electrodes (3×5 mm contact area). Electrically-induced neurogenic extravasation was prevented by using this high frequency stimulation regime which does not activate group III and IV masseter muscle afferent neurons [23]. Stimulation current was adjusted (5–7mA constant current) to produce a supramaximal tetanic muscle contraction. One hundred fifty milliseconds following activation of the masseter muscle, the mandible was displaced 25 degrees (jaw opening) at a rate of 0.6°/ms. Mandibular displacement was achieved by activating a stepping motor (1.8°/step; NMB Technologies, Chatsworth, CA) controlled by a custom Labview program (Labview, version 8.5, National Instruments, Austin, TX). Torque was measured using a torque sensor (model QWLC-8M Sensotec, Columbus, OH) and amplifier (model DV-05, Sensotec) while angular position of the mandible was monitored via a potentiometer. Mandibular displacement, torque and angular position data were synchronized using a custom Labview program. Signals were sampled at a rate of 2K Hz using a 16 bit analog to digital board (PCI-6221, National Instruments). Five sets of 100 eccentric muscle contractions were produced with a 5min rest between sets. A few initial experiments were conducted by manually displacing the mandible at a rate of 20 degrees per second to lengthen the masseter muscle. Rapid stretching of the masseter muscle was produced by displacing the mandible (25 degrees, 0.6°/ms) without muscle contraction. Concentric contraction of the masseter was produced by muscle stimulation without stretching.

### 2.2. Injection of complete Freund's adjuvant

For comparison to eccentric muscle contraction and stretching, muscle inflammation was produced in a separate group of animals by injecting complete Freund's adjuvant (CFA, Sigma F5881, 150µl of 0.5mg/ml heat killed *Mycobacterium tuberculosis* suspended in oil:saline (1:1) emulsion) into the masseter muscle.

### 2.3. Muscle edema

Edema was analyzed by harvesting the masseter muscle and determining the wet masseter muscle weight. The muscle was then placed in an oven, dried for 3d and weighed to determine the dry muscle weight. Muscle fluid content was defined as  $(\text{wet muscle weight} - \text{dry muscle weight}) / \text{wet muscle weight} \times 100$ .

### 2.4. Plasma extravasation

Leakage of Evans Blue dye (EB, E2129-10G Sigma) from the circulation was used to evaluate plasma extravasation. Animals were anesthetized with sodium pentobarbital and Evans Blue (50mg/kg in 0.2–0.3ml distilled H<sub>2</sub>O) was infused through the jugular vein. Fifteen minutes after injection of Evans Blue, animals were sacrificed and perfused with 0.9% saline. Masseter muscle tissue was diced, placed in an extraction solution (acetone and 35.2mM sodium sulfate in H<sub>2</sub>O) and shaken for 48h. Supernatant was then decanted and centrifuged at 10,000 rpm for 20min. The adsorbance of this solution was read at A<sub>620</sub> using a spectrophotometer. The dye content of each sample was compared to a standard curve of

known Evans Blue concentrations. The amount of Evans Blue in grams was calculated per gram of dry tissue.

## 2.5. Determination of myofiber membrane integrity

Muscle myofiber integrity was determined by injecting Evans Blue [55]. Evans Blue (1% in phosphate-buffered saline, pH 7.4; 1mg Evans Blue/10g body weight) was filtered (0.2 $\mu$ m) and injected intraperitoneally. After 24h, the masseter muscle was eccentrically contracted (500 contractions) or stretched (500 stretches). Twenty-four hours following EC or stretching the animals were decapitated and the muscles of mastication were removed, dissected into three portions (anterior, middle, posterior) and quick frozen by immersion in isopentane (-150°C) cooled by liquid nitrogen. Muscle specimens were cryosectioned (10 $\mu$ m) and coverslipped with aqueous mounting media (PermaFluor, Thermo). Muscle sections were then examined under epifluorescent illumination (excitation 535–550nm, barrier 565nm). Myofibers containing Evans Blue indicative of membrane disruption were readily identified by the presence of strong, homogeneous labeling within a myofiber. Disrupted myofibers were quantified by dividing the masseter muscle into three blocks and randomly selecting and analyzing a muscle section from each block. Images were collected from each entire muscle section (average=22.1 images/section) and thresholded (SigmaScan Pro). Myofibers with intensities 50% greater than background myofibers were considered to be Evans Blue positive myofibers. All myofibers above and below threshold were manually counted from each entire selected muscle section to determine the number of myofibers containing Evans Blue in each muscle section.

## 2.6. Histology and immunocytochemistry

Muscles were examined for signs of muscle damage and inflammation using histological and immunohistochemical techniques. Naive and contracted muscles were sectioned (12 $\mu$ m) and stained with hemotoxylin and eosin (H+E). Sections of the masseter muscle were randomly selected and myofibers in that section were quantitatively analyzed for myofiber area, shape, compactness, and average intensity using image analysis software (SigmaScan Pro 5.0, SPSS, Chicago, USA). Area was calculated as the sum of pixels within an object. Compactness is a numeric representation of the shape of an object as it moves from a circle to a line. Compactness was calculated as the perimeter squared divided by the area. Thus minimum compactness (i.e. a circle) is about 12.57 and as an object tends towards the shape of a line the value increases. The shape factor calculates circularity of a myofiber. The shape factor is calculated as  $\text{shape factor} = (4\pi \times \text{Area})/\text{perimeter}^2$ . Thus the shape factor of a perfect circle would equal 1.0 and a line would have a shape factor approaching 0.

The presence of inflammatory cells was examined using immunocytochemistry. Muscles were cryosectioned (15 $\mu$ m) onto slides and fixed in cold acetone for 2min. Sections were then washed in PBS (5–10min) and incubated in 1% H<sub>2</sub>O<sub>2</sub> in methanol for 30min at room temp. After washing in PBS, sections were incubated in normal horse serum (Vector, 2.5%) for 30min at room temperature. Sections were then incubated in either: mouse monoclonal anti-ED1 (1:50 Serotec MCA 341R); mouse monoclonal anti-ED2 (1:50 Serotec MCA342R) or granulocyte antibody for neutrophils (HIS) antibody (1:25 BD Pharmigen 550304) for 2h at room temperature in a humid chamber. Sections were then incubated in biotinylated anti-mouse (1:600, Vector Laboratories) for 30min in a humid chamber. After washing in PBS, sections were incubated in ABC (Vector ABC elite PK-6102, 1:400) for 30min at room temperature. Sections were then washed in PBS and rinsed in Tris buffer (pH 7.6) for 5min. Tissue sections were then incubated in diaminobenzidine (DAB, 0.02%) for 5min. Reactions were monitored under a microscope and terminated by dilution with PBS. Muscle sections were then dehydrated in graded alcohols and coverslipped (Permount). For each antibody, a control was conducted by incubating in PBST instead of the primary

antibody. These omission controls showed no staining. Rat spleen tissue was used as positive controls for HIS48, ED1, ED2 and showed large numbers of stained cells.

## 2.7. Enzyme-linked immunosorbent assay (ELISA)

Animals were decapitated and the masseter muscles dissected and minced with scissors. Muscles were then ground in RIPA buffer (Santa Cruz Biotechnology) containing protease inhibitor (complete, EDA-free, Roche) in a teflon glass homogenizer. Homogenates were centrifuged for 8min (15,000xg, 4°C) and the supernatant was saved for assay. Protein content was determined by the Bradford method (Bio-Rad). The cytokines were measured by two-antibody ELISA using biotin-streptavidin-peroxidase detection. Polystyrene plates (Maxisorb; Nunc) were coated with capture antibody in PBS overnight at 25°C. The plates were washed 4 times with 50mM Tris, 0.2% Tween-20, pH 7.0–7.5 and then blocked for 90min at 25°C with assay buffer (PBS containing 4% BSA and 0.01% Thimerosal, pH 7.4). The plates were washed 4 times and 50µl assay buffer was added along with 50µl of sample or standard prepared in assay buffer and incubated at 37°C for 2h. After washing 4 times, the plates were incubated with biotinylated detecting antibody for 1h at 25°C. The plates were washed 4 times and reacted with streptavidin-peroxidase polymer in casein buffer (RDI) at 25°C for 30min. Following 4 washes the plates were reacted with 100µl substrate (TMB; Dako) for approximately 10–30min at 25°C. The reaction was stopped with 100µl 2N HCl and the  $A_{450}$  was read on a microplate reader (Molecular Dynamics). Following subtraction of  $A_{650}$ , a curve was fit to the standards using a computer program (SoftPro; Molecular Dynamics) and cytokine concentration in each sample was calculated from the standard curve equation.

## 2.8. Behavioral assessment

Animals were tested for their response to mechanical stimulation of the masseter muscle region using a rigid von Frey filament coupled with a force transducer (Electrovonfrey, model no 2290, IITC, tip diameter 1.03mm). Animals were habituated using the methodology described by Ren [82] and a continuously variable force transducer with a fixed contact area was used to measure withdrawal thresholds. Initially animals were habituated to stand unrestrained on their hindpaws and lean on the experimenter's hand enclosed in a leather glove. Mechanical thresholds were then tested by probing the masseter muscle through the facial skin or the lateral edge of the hindpaw. The force needed to elicit a withdrawal of the head or foot was recorded following five stimulus presentations at approximately one 1min intervals and the mean values of the five readings were used for analysis.

## 2.9. Radioimmunoassay (RIA)

Trigeminal ganglia were harvested after rats were killed by decapitation. Since the somata of non-spindle masticatory muscle afferent neurons lie within the mandibular (V3) division of the trigeminal ganglion [23], V3 was separated from the ophthalmic and maxillary divisions of the trigeminal ganglion (V1/V2), frozen in dry ice and stored at – 80°C until processed. Ganglion samples were homogenized in RIA buffer (RK-BUR, Phoenix Pharmaceuticals, USA), and the homogenates were centrifuged for 10min at 5000xg at 4°C. Supernatants were then separated and total protein content in each sample determined by Bradford's method. The supernatant was then used for a CGRP assay in duplicate using an RIA kit according to the manufacturer's instructions (#RK-015-09, Phoenix Pharmaceuticals Inc.). The sensitivity was 32 pg/tube. The intra-assay variance was 5% while the inter-assay variance was 10% (n=5). The cross-reactivity for the antibody used was 100% for rat CGRP and 35.5% for human CGRP.

## 2.10. Quantitative reverse transcription polymerase chain reaction (qRT-PCR)

Rats were decapitated 24h after muscle contraction or stretching. In some experiments dantrolene sodium (100 $\mu$ M, 3.4 $\mu$ l in sterile saline) was intramuscularly injected to block muscle contraction [17] during electrical stimulation. Right and left trigeminal ganglia were dissected. The mandibular (V3) division of the trigeminal ganglion was dissected and frozen with dry ice. Total RNA was extracted using an Absolute RNA kit (Stratagene) that includes a DNase treatment. 200ng of total RNA was used to generate cDNAs in 15 $\mu$ l with a Superscript II system (Invitrogen, Carlsbad, CA) [53]. The concentration and quality of extracted RNA was determined using an Agilent BioAnalyzer 2100. RNA integrity was evaluated by electropherograms, the 28S/18s rRNA subunit ratio and the RNA integrity number (RIN) a proprietary Agilent Technologies algorithm [65]. cDNA was only synthesized if extracted RNA had a RIN greater than 7 and a 28s/18s ratio greater than 1.1. Real-time qPCR was performed with TaqMan primers and probes in the Fast Start Universal Probe Master (Rox) (Roche RMB-04913957001) on the ABI Prism 7000 Sequence Detector (Applied Biosystems). All TaqMan primers and probes with high efficiency were obtained from ABI (cat. no. Rn00569199 for rat CGRP; Rn00579301 for rat P2X<sub>3</sub>; 4352338E for rat GAPDH). Optimal concentrations were determined for single gene reaction (monoplex mode) in 50 $\mu$ L volume containing cDNAs equal to 6–26ng RNA. Cycling parameters were 95°C for 10min followed by 45 cycles of 95°C for 15s and 58–60°C for 1min. Detection of cDNA of interest was expressed as the amplification cycle at which the relevant PCR product was first detected [threshold cycle (C<sub>T</sub>)]. The relative quantification of fold changes of mRNA levels was calculated by the comparative C<sub>T</sub> method ( $\Delta\Delta$ C<sub>T</sub> method) (ABI User Bulletin 2) as described previously [8]. Each assay was run in triplicate. The express level of the GAPDH gene was measured by TaqMan primer and probe from the same cDNA pools and served as internal controls to normalize the CGRP signal.

## 2.11. Muscle afferent labeling and CGRP, P2X<sub>3</sub> immunocytochemistry

Masticatory muscle afferent neurons were labeled essentially as described previously [4]. Briefly, rats were anesthetized with 2% isoflurane. A 1mm incision was made in the skin overlying the masseter muscle using aseptic technique and several portions of the masseter muscle were injected with rhodamine-dextran (10,000 kDa, D-1817, Molecular Probes, USA, total 6–8 $\mu$ l) dissolved in sterile saline through a single penetration of the fascia overlying the muscle. Leakage of tracer was prevented by applying petroleum jelly over the point where the injection syringe penetrated the muscle fascia. All animals were closely monitored for any signs of pain or distress after recovery from anesthesia.

Four days after dextran was injected into the muscle, rats were sacrificed and perfused transcardially with saline followed by a mixture of 4% paraformaldehyde. Trigeminal ganglion were removed, cryoprotected by immersion in 30% sucrose and frozen sections (20–30 $\mu$ m) were cut. Sections were incubated in PBS with 0.4% Triton-X-100 (PBST) for 48h at 4°C with a rabbit polyclonal antibody against  $\alpha$ -CGRP (1:5,000 T4032, 1HC6006 Peninsula Labs, USA) or P2X<sub>3</sub> (1:1000 Chemicon). Sections were then incubated in biotinylated anti-rabbit or anti-guinea pig anti-serum (1:200, ABC Elite kit, Vector Labs, USA) for 1h at room temperature. Sections were then incubated in fluorescein isothiocyanate (FITC) conjugated to avidin (1:400, Vector) for 1h at room temperature. Sections were mounted using an aqueous mounting medium (PermaFluor, Shandon, USA). Non-specific labeling for all peptide antibodies was evaluated previously following preadsorption and after omission of primary antibodies [4].

Ganglion sections were examined using wide-field epifluorescent illumination (Nikon Eclipse E800 microscope) with filters for rhodamine (excitation wavelength (ex) 528–553nm, barrier filter (bf) 600–660nm), FITC (ex 465–495nm, bf 515–555nm), and a dual

filter for FITC/rhodamine (ex 478–494nm and 535–570nm, bf 523–604nm). Rhodamine-labeled neurons and neurons double-labeled with both rhodamine and FITC were tallied manually with no knowledge of experimental history (i.e. blinded). Only neurons with a discernable nucleus and unambiguous labeling were included in the analysis. Since muscle afferent neurons are not uniformly distributed throughout the ganglia, neurons in all sections from each ganglion were counted to avoid potential sampling errors.

## 2.12. Statistical analysis

All data were initially tested for normality (Kolmogorov-Smirnov test) and equal variance (Sigma Stat, Jandel). Normally distributed data with equal variance were tested with parametric statistics (t-test, ANOVA followed by a Holm-Sidak *post-hoc* test). Non-normally distributed data or data with unequal variance were tested with non-parametric methods (Mann-Whitney rank sum test, Kruskal Wallis ANOVA on ranks followed by Dunn's method for multiple comparisons [25] or Friedman repeated measures ANOVA on ranks). A probability level of 0.05 was chosen for hypothesis testing. Actual *p*-values are reported for further evaluation.

## 3. Results

### 3.1. Muscle contraction

Pre-activation of the masseter muscle typically generated about 10Nmm torque (Fig. 1). Torque then increased during mandibular and muscle displacement reaching a peak as movement ceased. Torque developed during muscle contraction ranged from an initial mean of 189Nmm for the first contraction with a gradual decrease during subsequent contractions to a mean of 118Nmm for the last contraction. In the initial experiments the mandible was manually displaced to create eccentric contraction. Myofiber damage was less extensive following manual mandibular movement although no significant differences were apparent in other parameters.

### 3.2. Muscle edema

Eccentrically contracted muscles contained significantly more fluid than non-contracted muscles indicating that EC produced edema. Specifically, eccentrically contracted masseter muscles contained 2.8% more fluid than non-contracted muscles which was a significant increase in intramuscular fluid (Table 1; t-test  $p=0.038$ ,  $n=7$  animals, 14 muscles).

### 3.3. Plasma extravasation

The amount of Evans Blue ( $\mu\text{g/g}$  dry tissue) was significantly increased in the masseter muscle 1d after eccentric masseter muscle contraction (Fig. 2; one-way ANOVA on ranks followed by Dunn's method,  $p=0.014$ , naive  $n=26$ , 4h  $n=7$ , 1d  $n=13$ , 2d  $n=6$ , 4d  $n=12$ ). In contrast, no significant change in Evans Blue was found in the skin overlying the masseter muscle after eccentric masseter muscle contraction (Fig. 2; one-way ANOVA,  $p=0.449$ , naive  $n=28$ , 4h  $n=7$ , 1d  $n=11$ , 2d  $n=6$ , 4d  $n=10$ ) demonstrating that the stimulation evoked muscle inflammation without inflammation of the overlying skin. A significant increase in Evans Blue was found in the stretched masseter muscle (one-way ANOVA,  $p=0.05$ , naive  $n=25$ , 4h  $n=11$ , 1d  $n=15$ , 2d  $n=9$ , 4d  $n=11$ ).

### 3.4. Myofiber membrane damage

Frequent, scattered myofibers containing Evans Blue indicative of myofiber damage (Fig. 3) were found in masseter muscles which had been eccentrically contracted. Disrupted myofibers were not adjacent to each other and were not obviously compartmentalized within the muscle. These methodology used to quantify Evans Blue muscle fibers was initially

tested for reproducibility by counting five randomly selected sections from the same eccentrically-contracted muscle. These measurements yielded an average of 11.8% infiltrated Evans Blue muscle fibers (range 6 – 15.1%, SD=3.5, n=5 sections). Quantitative analysis of muscle sections (average of 2062 myofibers analyzed per section) from eccentrically-contracted masseter muscles from different animals showed that an average of 12.5% of masseter muscle myofibers were infiltrated by Evans Blue (n=5 animals, range 7.2%–16.1%, SD=3.4). In animals injected with Evans Blue but not subjected to EC (n=2), Evans Blue was confined to the extracellular space surrounding individual myofibers (Fig 3). In some animals injected with Evans Blue the masseter muscle was injected with CFA. Evans Blue in these animals was confined to the extracellular space surrounding myofibers and showed no evidence of myofiber membrane disruption (n=2)(Fig. 3). In rapidly stretched masseter muscle a small number of myofibers were disrupted (mean=4.9%, range 1.0%–12.6%, SD=4.8, n=5).

### 3.5. Muscle histology myofiber morphology

Quantitative analysis of histological muscle sections revealed that myofibers in eccentrically contracted muscles exhibited signs of myofiber damage. The area of myofibers from eccentrically contracted muscles was significantly larger than myofibers within control muscles (n=5 animals Mann-Whitney rank sum test  $p<0.001$ , control n=496 myofibers median 3838.5 $\mu\text{m}^2$ , contracted n=499 myofibers median=6107.00 $\mu\text{m}^2$ ). Eccentrically contracted myofibers were more circular and more compact than control myofibers (circularity: n=5 animals, Mann-Whitney rank sum test  $p<0.001$ , control n=496 myofibers median=0.72, EC n=499 myofibers, median=0.79; compactness: n=5 animals, Mann-Whitney rank sum test  $p<0.001$ , control n=496 myofibers, median=17.55, EC n=499 myofibers, median=16.01).

### 3.6. Inflammation and immunocytochemistry

Clear evidence of muscle inflammation was present following EC. Muscle sections stained with hematoxylin and eosin showed marked evidence of inflammatory cell infiltration (Fig 4A, control n=5; contraction n=12). Some myofibers exhibited evidence of focal invasion of muscle fibers (Fig. 4B, C) while others exhibited clear signs of myofiber swelling (Fig 4D asterisk). Immunocytochemistry was used to further characterize inflammation (control n=5, 1d post-contraction n=5, 2d post-contraction n=5, 4d post-contraction n=5). Neutrophils visualized with HIS48 antibody were found sparsely scattered throughout the masseter muscle 1 to 4d after EC. Neutrophils were typically located in the extracellular space and myofibers were very rarely infiltrated by neutrophils. Quantitative analysis of muscle harvested 1d following EC demonstrated that neutrophils were significantly increased (mean HIS48<sup>+</sup> cells/mm<sup>3</sup>; control=1691 n=5, contracted 3614 n=5, t-test  $p<0.05$ ). Myofibers were infiltrated by ED1 macrophages within 2d after contraction. Four days after contraction ED1 macrophages were scattered throughout contracted muscles with numerous myofibers infiltrated with ED1 macrophages. Since ED1 macrophages were the most numerous inflammatory cell examined (Fig. 4C,D), they were quantified and found to be significantly increased following EC (control=217 ED1 cells/mm<sup>3</sup> n=5, contracted=17,322 ED1 cells/mm<sup>3</sup>, n=5,  $p<0.001$ ). A few ED2 macrophages were found 1d after EC. Two days after contraction, ED2 macrophages were much more numerous and by 4d after EC ED2 macrophages were plentiful (Fig. 4E).

Injection of CFA into the masseter muscle (n=3) produced a markedly different inflammatory response than EC. In contrast to the focal inflammation with selected myofiber infiltration, CFA produced a massive, non-specific inflammatory response in the muscle. Granulocytes and both ED1 and ED2 macrophages were ubiquitous (Fig. 4F). In



addition CFA produced large vacuoles in the muscle. This type of massive, non-specific inflammation with vacuoles was never observed following EC.

### 3.7. Cytokines

Prominent pro-inflammatory cytokines were significantly increased in the masseter muscle 24h following EC and stretching. A significant increase in intramuscular interleukin-6 (IL-6) was found 24h following EC and stretching using ELISA (naive 1.50 pg/mg protein, contracted 2.53 pg/mg protein, one-way ANOVA,  $p=0.032$ ,  $n=18$ , 8 naive, 5 contracted, 5 stretched). Intramuscular tumor necrosis factor alpha (TNF- $\alpha$ ) was also significantly increased 24h following EC and stretching (naive 0.098 pg/mg protein, contracted 0.203 pg/mg protein, stretched 0.242 pg/mg protein, one-way ANOVA  $p=0.019$ ,  $n=19$ , 9 naive, 5 contracted, 5 stretched). Levels of interleukin-1 $\beta$  (IL-1 $\beta$ ) in the masseter were significantly increased following EC but not stretching (naive 0.518 pg/mg protein, contracted 0.820 pg/mg protein, one-way ANOVA  $p=0.046$ ,  $n=18$ , 8 naive, 5 contracted, 5 stretched). The cytokine vascular endothelial growth factor (VEGF) was also significantly increased following EC but not stretching of the masseter muscle (naive 0.633 pg/mg protein, contracted 1.19 pg/mg protein, stretched 1.03 pg/mg protein, one-way ANOVA  $p=0.038$ ,  $n=17$ , 6 naive, 6 contracted, 5 stretched).

### 3.8. Mechanical hyperalgesia

The mechanical threshold which evoked a head withdrawal was tested in rats prior to and following eccentric, concentric contraction and stretching of the masseter muscle. Following a single bout of EC (500 contractions), the head withdrawal threshold was significantly reduced when a force was applied to the region of the masseter muscle (one-way repeated measures ANOVA,  $n=10$ ,  $p<0.001$ ). This mechanical hyperalgesia peaked 4h following EC and persisted for 4d (Fig. 5, Holm-Sidak method of multiple comparisons). No reduction in head withdrawal threshold was found on the contralateral head, ipsilateral or contralateral hindlimb following EC (Friedman repeated measures one-way ANOVA on ranks, contralateral face:  $n=10$ ,  $p<0.001$ ; ipsilateral hindpaw:  $n=10$ ,  $p<0.001$ ; contralateral hindpaw:  $n=10$ ,  $p<0.001$ ). In some cases analysis of variance tests were significant. The Holm Sidak method of multiple comparisons revealed that 12d after contraction there was a slight, but significant, increase in the contralateral head withdrawal threshold. Rapid stretching of the masseter muscle without muscle contraction produced a significant drop in the head withdrawal threshold from 4h through 2d (one-way repeated measures ANOVA followed by Holm-Sidak method  $p<0.001$ ,  $n=6$ ). Stretching had no effect on hindpaw withdrawal threshold (Friedman repeated measures one-way ANOVA on ranks, right hindpaw  $p=0.07$  left hindpaw  $p=0.07$ ,  $n=6$ ). Contracting the masseter without stretching the muscle also did not alter the head withdrawal threshold (Friedman one-way repeated measures ANOVA on ranks; ipsilateral face  $p=0.29$ ; contralateral face  $p=0.21$ ; ipsilateral hindlimb  $p=0.19$ ; contralateral hindlimb  $p=0.20$ , pretest  $n=6$ , contract  $n=2$ ).

Four consecutive bouts of eccentric masseter muscle contraction (500 contractions per day) produced a more prolonged reduction in the ipsilateral head withdrawal threshold than was evoked by a single bout of EC. Following four bouts of EC the withdrawal threshold was significantly reduced from 4h through 7d (Fig. 6, one-way repeated measures ANOVA,  $n=4$ ,  $p<0.001$ , Holm Sidak method). There was however no difference in the maximum percent reduction in withdrawal threshold produced by one versus multiple bouts of EC (t-test,  $p=0.21$ ). In addition, four bouts of contraction produced a reduction in the contralateral head withdrawal threshold 4h following EC through 2d (one-way repeated measures ANOVA  $n=4$ ,  $p<0.001$ , Holm Sidak method). No reduction in withdrawal threshold was detected in the ipsilateral hindpaw (one-way repeated measures ANOVA,  $n=4$ ,  $p=0.003$ ) or contralateral hindpaw (Friedman one-way repeated measures ANOVA on ranks,  $n=4$ ,

$p=0.005$ ). A significant increase was found in the ipsilateral hindpaw 14d following contraction (Dunn's method).

The absolute values for evoking head withdrawal responses are slightly higher than reported by Ren [83] since we are using a larger probe (1.03mm) than an equivalent von Frey filament (0.55mm) to preferentially stimulate deeper tissue [97]. Even higher thresholds are reported when larger probes are utilized [24,89].

### 3.9. CGRP content in the trigeminal ganglion

We used RIA to investigate whether there was a change in CGRP within the trigeminal ganglion following EC. Since the somata of non-spindle masticatory muscle afferent neurons lie within the mandibular (V3) division of the trigeminal ganglion [23], we separated the V1/V2 region of the ganglion from the V3 division where masseter muscle afferent somata are located. In naive animals ( $n=5$ ) mean immunoreactive CGRP (iCGRP) in V3 was 0.799 pg/ $\mu$ g. Twenty four hours after EC iCGRP was 0.500 pg/ $\mu$ g in the ipsilateral V3 ( $n=4$ ) versus 0.669 pg/ $\mu$ g in the contralateral V3 ( $n=4$ ). The iCGRP level in V3 from the side of the eccentrically contracted masseter muscle is significantly lower than from either the naive V3 or the contralateral V3 (one-way ANOVA followed by Holm-Sidak method,  $p=0.43$ ). No significant differences were found between naive V1/V2 and V1/V2 from EC animals or between naive V1/V2 and naive V3. ( $n=4$  for each group).

### 3.10. CGRP, P2X<sub>3</sub> gene expression

High quality RNA was extracted from the trigeminal ganglion (28s/18s ratio mean=8.9; RNA integrity number mean=8.9) and used to produce cDNA. The level of CGRP mRNA in the mandibular division of the trigeminal ganglion (V3) was significantly higher in the ipsilateral V3 following EC and muscle stretching (Fig. 7, one-way ANOVA  $p=0.029$  followed by Holm-Sidak method, naive  $n=8$ ; EC  $n=7$ ; stretched  $n=7$ ). The level of P2X<sub>3</sub> mRNA in the mandibular division of the trigeminal ganglion (V3) was significantly higher in the ipsilateral V3 following EC but not muscle stretching (one-way ANOVA  $p=0.021$  followed by Holm-Sidak method, naive  $n=8$ , EC  $n=7$ , stretching  $n=5$ ).

To investigate the possibility that electrical stimulation of peripheral nerves could modulate ganglionic CGRP and P2X<sub>3</sub> expression, dantrolene was injected into the masseter muscle and electrical stimulation ( $n=500$ ) was applied in the same manner used for EC. No muscle contraction was visible following intramuscular dantrolene injection. No change in ganglionic CGRP or P2X<sub>3</sub> mRNA was found in V3 following electrical stimulation of the masseter muscle while muscle contraction was blocked using intramuscular injection of dantrolene (CGRP: t-test,  $p=0.27$ , naive  $n=8$ , stimulation without contraction  $n=2$ ; P2X<sub>3</sub> t-test  $p=0.72$ , naive  $n=8$ , stimulation without contraction  $n=2$ ).

### 3.11. Percentage of CGRP, P2X<sub>3</sub> muscle afferent neurons

We investigated whether EC modulated CGRP expression in muscle afferent neurons by quantifying the percentage of trigeminal ganglion neurons labeled from the masseter muscle which were immunopositive for CGRP. Neurons labeled with rhodamine from muscle injections and CGRP immunopositive neurons were readily distinguishable and comparable to previous studies [4]. Previous studies show that intramuscular injection of dextran does not produce substantial muscle inflammation [1]. No significant differences were found in the number of CGRP containing muscle afferent neurons 2d or 12d following EC (Fig. 8A, one-way ANOVA  $p=0.502$ ; control mean=32.21,  $n=6$ ; 2d after contraction mean=37.22,  $n=5$ ; 12d following contraction mean=38.00,  $n=8$ ). P2X<sub>3</sub>-immunopositive muscle afferent neurons were significantly increased at both 2d and 12d following EC (one-way ANOVA  $p=0.001$  followed by Holm-Sidak method, naive  $n=10$ , EC (2d)  $n=5$ , EC (12d)  $n=6$ ).

Following rapid muscle stretching, no difference was found in the number of CGRP-immunopositive muscle afferent neurons 2 or 12d following EC (one-way ANOVA  $p=0.770$ , naive  $n=6$ , stretch-2d  $n=5$ , stretch 4d  $n=5$ ). In contrast to this, P2X<sub>3</sub>-immunopositive muscle afferent neurons were significantly increased at both 2d and 12d following stretching (one-way ANOVA  $p=0.001$  followed by Holm-Sidak method, naive  $n=13$ , stretching (2d)  $n=6$ , stretching (12d)  $n=5$ ).

#### 4. Discussion

We have utilized non-invasive, movement-based models to produce muscle inflammation and mechanical hyperalgesia. These models produce selective: myofiber damage, myonecrosis and inflammatory infiltration, all processes reported following voluntary eccentric movement [10]. Eccentric exercise and ballistic stretching in humans also produces muscle soreness [90,104] consistent with the mechanical hyperalgesia found in this study. Most previous models of muscle pain are invasive and typically activate only a subset of nociceptive receptors (e.g. mustard oil, capsaicin) [9,51]. Models such as CFA evoke a massive inflammatory response with tissue erosion which does not correspond to known muscle pathologies and decrease pro-angiogenic and neurotrophic factors [103]. In addition, none of these previous models incorporate characteristic features of muscle such as contractility and movement.

Eccentric muscle contractions and stretching were produced using mandibular displacements within the normal physiological range for rats [105]. Since masseter muscle sarcomeres lengthen during jaw opening [67,68,79], ECs were produced when the muscle was entirely on the descending limb of the length-tension relationship. This relationship and the pre-activation we employed prior to muscle lengthening facilitate muscle injury [13,52,56]. Force and torque measured during the initial masseter contraction are similar to values generated by rat hindlimb muscles [33,56]. A one third reduction in force occurred between the initial and last muscle contraction of each experiment. This reduction is attributable to both fatigue and muscle injury, although injury produced by EC is likely independent of fatigue [64]. While a substantial number of muscle contractions were used in this study, other masseter studies have employed more ECs [32] or contraction for 30min per day for 14d [89] and hindlimb studies have used 100–500 ECs [35,46,47,95,96].

Increased intramuscular fluid content and Evans Blue indicate that muscle edema and plasma extravasation were present following EC. Cutaneous neurogenic inflammation was prevented by anesthetizing the skin overlying the masseter and utilizing brief stimulation pulses to avoid activation of C-fibers. Furthermore, electrical stimulation of nerves evokes only minimal intramuscular plasma extravasation [61]. Previous hindlimb studies demonstrate that EB can be used as a marker for myofiber disruption [11,38,55]. Scattered myofibers containing EB were evident in EC and stretched muscles. Additional indications of myofiber damage include significantly larger, more circular and compact myofibers after contraction consistent with hindlimb studies [75]. Large, type II hindlimb myofibers are preferentially damaged in eccentric exercise and electrically-induced eccentric muscle contraction [7,31,45]. Since fiber types vary in many aspects (e.g. myosin isoforms, glycogen content, abundance of oxidative enzymes), preferential disruption of large myofibers is likely to expose peripheral muscle nerves to a distinctly different extracellular milieu than non-selective muscle pain models or hindlimb unloading/reloading [102].

Neutrophils were significantly increased in the masseter muscle 1d following EC similar to hindlimb muscles [60,75,100]. It has been proposed that neutrophils exacerbate contraction-induced muscle injury and impair the recovery of muscle function [75]. ED1 macrophages infiltrated myofibers 2–4d following EC as in hindlimb studies [60]. ED1 macrophages are

the first macrophage subpopulation to infiltrate muscle following EC and are thought to participate in muscle repair [59]. While the density of ED1 macrophages was substantially greater than that following hindlimb EC [60], it is comparable to densities following downhill running and hindlimb reloading [30,100]. The scattered pattern of ED1 myofiber infiltration is similar to that of myofibers containing EB following EC, likely indicating that myofibers damaged by EC are later phagocytized. Four days post-contraction, ED2 macrophages are numerous and often present within spaces previously occupied by myofibers. ED2 macrophages are thought to contribute to muscle regeneration by causing satellite cell activation and myoblast proliferation [60]. In contrast to the prominent inflammation found in this study, Fujii and co-workers [32] report minimal inflammation after EC likely due to the very slow rate of muscle stretch and lack of muscle pre-activation.

Pro-inflammatory cytokines are significantly increased within the masseter muscle following EC and stretching. Intramuscular IL-1 $\beta$ , TNF- $\alpha$  and IL-6 [15,22,84] as well as IL-6 mRNA [92] are also elevated following limb muscle EC. In the masseter muscle, IL-6 may be regulated by contraction since IL-6 mRNA increases when the muscle is electrically stimulated and suppressed when contraction is disrupted [72] although metabolic roles are also proposed for muscle-derived IL-6 [74]. A significant increase in intramuscular VEGF occurred following EC. This proangiogenic factor also increases within muscle following exercise [44,50,85] and is thought to be related to contraction-induced skeletal muscle angiogenesis. VEGF is also a neurotrophic factor selectively expressed in small-diameter neurons [91]. The intramuscular cytokine profile following EC represents one of the unique features of the EC pain model since intramuscular injection of CFA decreases VEGF [103] and carageenan does not elevate TNF- $\alpha$  [54].

Eccentric contraction and rapid stretching of the masseter muscle consistently produced craniofacial mechanical hyperalgesia. Multiple bouts of EC produce a more prolonged mechanical hyperalgesia lasting up to 7d. Muscle contraction without stretching did not produce hyperalgesia indicating that the behavioral responses are not due to muscle contraction alone nor are they due to stress induced by the experimental procedure. Only minimal mechanical hyperalgesia was found within 48h following 15 consecutive days of concentric masseter muscle contraction [89] suggesting that EC and rapid stretching more readily produce hyperalgesia. In hindlimb muscle, mechanical withdrawal thresholds are reduced for 3d after a single bout of 500–600 ECs [32,95]. Previous human studies indicate that muscle soreness produced by eccentric movement has a similar time course as the mechanical hyperalgesia found in this study [20,34,104].

Levels of CGRP within the ipsilateral mandibular division of the trigeminal ganglion were reduced 24h following EC. This result differs markedly from previous studies of muscle pain. Intramuscular injection of CFA elevated ganglionic iCGRP within 1h and iCGRP remained elevated for 12d [5]. Similarly adjuvant-induced jaw joint inflammation elevated CGRP levels within 6h and CGRP remained elevated for 10d [43]. We interpret the decrease in ganglionic CGRP following EC as a release of CGRP from ganglionic, presumably muscle afferent, neurons. CGRP mRNA increased 24h following EC and by 2d, the number of CGRP-containing muscle afferent neurons was comparable to naive animals. These data suggest that CGRP is initially released following EC and then gene expression is upregulated to replenish CGRP within muscle afferent neurons. It is likely that this CGRP release evoked by EC potentiates neurogenic extravasation since CGRP vasodilates blood vessels in muscle [70] and mediates neurogenic inflammation [12]. Unlike studies using CFA [5], we found no increase in the number of CGRP-muscle afferent neurons following EC or stretching. P2X<sub>3</sub> gene expression was increased 24h following EC and the number of P2X<sub>3</sub> muscle afferent neurons was significantly higher than naive 2d through 12d after EC. *In vitro* studies report that CGRP can upregulate P2X<sub>3</sub> expression in trigeminal neurons

[28], thus the release of CGRP evoked by EC may contribute to the increased expression of P2X<sub>3</sub> reported here *in vivo*. P2X channels on nociceptors can be activated by the release of ATP from nearby cells [19]. The concentration of ATP within myofibers is approximately 10mM [93], a concentration which readily activates muscle primary afferent neurons *in vivo* [81]. Thus we propose that P2X<sub>3</sub> channels on muscle afferent neurons are activated by ATP released from undamaged myofibers and myofibers damaged by eccentric exercise and that the increased P2X<sub>3</sub> expression evoked by EC further enhances the responsiveness of these neurons to repetitive bouts of EC. In comparison to EC, P2X<sub>3</sub>-immunopositive muscle afferents were increased for several days following intramuscular injection of CFA but then decreased at 12d [3]. Thus both CGRP and P2X<sub>3</sub> expression following EC differ markedly from that evoked by adjuvant injection. The number of P2X<sub>3</sub> muscle afferent neurons is also increased following 15d of electrically contracting the masseter muscle [89]. Here, we show that electrical stimulation without muscle contraction does not alter CGRP or P2X<sub>3</sub> gene expression, indicating that increased gene expression following electrically evoked muscle contraction is not due to antidromic stimulation of peripheral nerves.

Muscle stretching increased CGRP gene expression within 24h. Two days following stretching, the number of CGRP muscle afferents was comparable to naive animals. While CGRP is strongly implicated in nociception and inflammation [43,66,106], it is also implicated in healing and thought to interact with VEGF to increase angiogenesis [99]. Thus the modulation of CGRP by EC and stretching may serve multiple functions including muscle repair. Stretching did not alter P2X<sub>3</sub> mRNA levels at 24h but increased the number of P2X<sub>3</sub> muscle afferent neurons for 12d. Perhaps the difference in gene expression evoked by stretching compared with EC is attributable to the extensive damage to interstitial connective tissue produced by rapid stretching [101] which differs from contraction-induced muscle injury.

This study shows that neuropeptides and nociceptive receptors are modulated in functionally relevant ways by movement-based models which incorporate unique muscle features such as contractility and myofiber heterogeneity.

## Acknowledgments

We thank E Wade for technical assistance, R Lovering for help with the muscle displacement system and J Michael for help with electronics and LabView programming. This work was supported by NIH grants DE15386 and DE10132 to DD. The authors declare that they do not have a conflict of interest with any of the work presented in this manuscript.

## Reference List

1. Ambalavanar, R.; Dessem, D. The involvement of calcitonin gene related peptide in deep tissue nociception. In: Farley, Elizabeth P., editor. Progress in Neuropeptide Research. New York: NOVA; 2007.
2. Ambalavanar R, Dessem D. Emerging peripheral receptor targets for deep-tissue craniofacial pain therapies. J Dent Res 2009;88:201–211. [PubMed: 19329451]
3. Ambalavanar R, Moritani M, Dessem D. Trigeminal P2X3 receptor expression differs from dorsal root ganglion and is modulated by deep tissue inflammation. Pain 2005;117:280–291. [PubMed: 16153775]
4. Ambalavanar R, Moritani M, Haines A, Hilton T, Dessem D. Chemical phenotypes of muscle and cutaneous afferent neurons in the rat trigeminal ganglion. J Comp Neurol 2003;460:167–179. [PubMed: 12687682]
5. Ambalavanar R, Moritani M, Moutanni A, Gangula P, Yallampalli C, Dessem D. Deep tissue inflammation upregulates neuropeptides and evokes nociceptive behaviors which are modulated by a neuropeptide antagonist. Pain 2006;120:53–68. [PubMed: 16359792]

6. Ambalavanar R, Yallampalli C, Yallampalli U, Dessem D. Injection of adjuvant but not acidic saline into craniofacial muscle evokes nociceptive behaviors and neuropeptide expression. *Neuroscience* 2007;149:650–659. [PubMed: 17928159]
7. Asp S, Dugaard JR, Kristiansen S, Kiens B, Richter EA. Exercise metabolism in human skeletal muscle exposed to prior eccentric exercise. *J Physiol* 1998;509:305–313. [PubMed: 9547403]
8. Bai G, Ambalavanar R, Wei D, Dessem D. Downregulation of selective microRNAs in trigeminal ganglion neurons following inflammatory muscle pain. *Mol Pain* 2007;3:15. [PubMed: 17559665]
9. Bautista DM, Jordt SE, Nikai T, Tsuruda PR, Read AJ, Poblete J, Yamoah EN, Basbaum AI, Julius D. TRPA1 mediates the inflammatory actions of environmental irritants and proalgesic agents. *Cell* 2006;124:1269–1282. [PubMed: 16564016]
10. Beaton LJ, Tarnopolsky MA, Phillips SM. Contraction-induced muscle damage in humans following calcium channel blocker administration. *J Physiol* 2002;544:849–859. [PubMed: 12411528]
11. Boppart MD, Burkin DJ, Kaufman SJ. Alpha7beta1-integrin regulates mechanotransduction and prevents skeletal muscle injury. *Am J Physiol Cell Physiol* 2006;290:C1660–C1665. [PubMed: 16421207]
12. Brain SD, Tippins JR, Morris HR, MacIntyre I, Williams TJ. Potent vasodilator activity of calcitonin gene-related peptide in human skin. *J Invest Dermatol* 1986;87:533–536. [PubMed: 2428885]
13. Brooks SV, Zerba E, Faulkner JA. Injury to muscle fibres after single stretches of passive and maximally stimulated muscles in mice. *J Physiol* 1995;488:459–469. [PubMed: 8568684]
14. Bulling DGS, Kelly D, Bond S, McQueen DS, Seckl JR. Adjuvant-induced joint inflammation causes very rapid transcription of beta-preprotachykinin and alpha-CGRP genes in innervating sensory ganglia. *J Neurochem* 2001;77:372–382. [PubMed: 11299299]
15. Cannon JG, St Pierre BA. Cytokines in exertion-induced skeletal muscle injury. *Mol Cell Biochem* 1998;179:159–167. [PubMed: 9543358]
16. Carleson J, Lundeberg T, Appelgren B. Muscle and brain changes of calcitonin gene-related peptide in experimentally induced unilateral rat masseter myositis. *J Orofac Pain* 2004;18:246–252. [PubMed: 15509004]
17. Cherednichenko G, Ward CW, Feng W, Casbrales E, Michaelson L, Samsó M, Lopez JR, Allen PD, Pessah IN. Enhanced excitation-coupled calcium entry in myotubes expressing malignant hyperthermia mutation R163C is attenuated by dantrolene. *Mol Pharmacol* 2008;73:1203–1212. [PubMed: 18171728]
18. Clark, GT. Treatment of myogenous pain and dysfunction. In: Laskin, DM.; Greene, CS.; Hylander, WL., editors. *TMDs; An evidence-based approach to diagnosis and treatment*. Chicago: Quintessence Publishing Co, Inc; 2006.
19. Cook SP, McCleskey EW. Cell damage excites nociceptors through release of cytosolic ATP. *Pain* 2002;95:41–47. [PubMed: 11790466]
20. Crameri RM, Aagaard P, Qvortrup K, Langberg H, Olesen J, Kjaer M. Myofibre damage in human skeletal muscle: effects of electrical stimulation versus voluntary contraction. *J Physiol* 2007;583:365–380. [PubMed: 17584833]
21. Curatolo M, Bogduk N. Pharmacologic pain treatment of musculoskeletal disorders: current perspectives and future prospects. *Clin J Pain* 2001;17:25–32. [PubMed: 11289086]
22. Davis JM, Murphy EA, Carmichael MD, Zielinski MR, Groschwitz CM, Brown AS, Gangemi JD, Ghaffar A, Mayer EP. Curcumin effects on inflammation and performance recovery following eccentric exercise-induced muscle damage. *Am J Physiol Regul Integr Comp Physiol* 2007;292:R2168–R2173. [PubMed: 17332159]
23. Dessem D, Moritani M, Ambalavanar R. Nociceptive craniofacial muscle primary afferent neurons synapse in both the rostral and caudal brain stem. *J Neurophysiol* 2007;98:214–223. [PubMed: 17493918]
24. Dina OA, Green PG, Levine JD. Role of interleukin-6 in chronic muscle hyperalgesic priming. *Neuroscience* 2008;152:521–525. [PubMed: 18280048]
25. Dunn OJ. Multiple contrasts using rank sums. *Technometrics* 1964;6:241–252.

26. Ernberg M, Lundeberg T, Kopp S. Pain and allodynia/hyperalgesia induced by intramuscular injection of serotonin in patients with fibromyalgia and healthy individuals. *Pain* 2000;85:31–39. [PubMed: 10692600]
27. Evans M, Morine K, Kulkarni C, Barton ER. Expression profiling reveals heightened apoptosis and supports fiber size economy in the murine muscles of mastication. *Physiol Genomics* 2008;35:86–95. [PubMed: 18593863]
28. Fabbretti E, D'Arco M, Fabbro A, Simonetti M, Nistri A, Giniatullin R. Delayed upregulation of ATP P2X3 receptors of trigeminal sensory neurons by calcitonin gene-related peptide. *J Neurosci* 2006;26:6163–6171. [PubMed: 16763024]
29. Fock S, Mense S. Excitatory effects of 5-hydroxytryptamine, histamine and potassium ions on muscular group IV afferent units: a comparison with bradykinin. *Brain Res* 1976;105:459–469. [PubMed: 1260457]
30. Frenette J, St-Pierre M, Cote CH, Mylona E, Pizza FX. Muscle impairment occurs rapidly and precedes inflammatory cell accumulation after mechanical loading. *Am J Physiol Regul Integr Comp Physiol* 2002;282:R351–R357. [PubMed: 11792643]
31. Friden J, Sjøstrom M, Ekblom B. Myofibrillar damage following intense eccentric exercise in man. *Int J Sports Med* 1983;4:170–176. [PubMed: 6629599]
32. Fujii Y, Ozaki N, Taguchi T, Mizumura K, Furukawa K, Sugiura Y. TRP channels and ASICs mediate mechanical hyperalgesia in models of inflammatory muscle pain and delayed onset muscle soreness. *Pain* 2008;140:292–304. [PubMed: 18834667]
33. Garma T, Kobayashi C, Haddad F, Adams GR, Bodell PW, Baldwin KM. Similar acute molecular responses to equivalent volumes of isometric, lengthening, or shortening mode resistance exercise. *J Appl Physiol* 2007;102:135–143. [PubMed: 17008438]
34. Gibson W, rendt-Nielsen L, Graven-Nielsen T. Delayed onset muscle soreness at tendon-bone junction and muscle tissue is associated with facilitated referred pain. *Exp Brain Res* 2006;174:351–360. [PubMed: 16642316]
35. Gibson W, Arendt-Nielsen L, Taguchi T, Mizumura K, Graven-Nielsen T. Increased pain from muscle fascia following eccentric exercise: animal and human findings. *Exp Brain Res* 2009;194:299–308. [PubMed: 19156402]
36. Glaros AG, Williams K, Lausten L. The role of parafunctions, emotions and stress in predicting facial pain. *J Am Dent Assoc* 2005;136:451–458. [PubMed: 15884314]
37. Graham DY, Opekun AR, Willingham FF, Qureshi WA. Visible small-intestinal mucosal injury in chronic NSAID users. *Clin Gastroenterol Hepatol* 2005;3:55–59. [PubMed: 15645405]
38. Hamer PW, McGeachie JM, Davies MJ, Grounds MD, Evans Blue Dye as an in vivo marker of myofibre damage: optimising parameters for detecting initial myofibre membrane permeability. *J Anat* 2002;200:69–79. [PubMed: 11837252]
39. Harriott AM, Dessem D, Gold MS. Inflammation increases the excitability of masseter muscle afferents. *Neuroscience* 2006;141:433–442. [PubMed: 16690218]
40. Hedenberg-Magnusson B, Ernberg M, Koop S. Symptoms and signs of temporomandibular disorders in patients with fibromyalgia and local myalgia of the temporomandibular system. *Acta Odontol Scand* 1997;55:344–349. [PubMed: 9477026]
41. Ho TW, Mannix LK, Fan X, Assid C, Furtek C, Jones CJ, Lines CR, Rapoport AM. Randomized controlled trial of an oral CGRP antagonist, MK-0974, in acute treatment of migraine. *Neurology* 2008;70:1304–1312. [PubMed: 17914062]
42. Hoheisel U, Reinohl J, Unger T, Mense S. Acidic pH and capsaicin activate mechanosensitive group IV muscle receptors in the rat. *Pain* 2004;110:149–157. [PubMed: 15275762]
43. Hutchins B, Spears R, Hinton RJ, Harper RP. Calcitonin gene-related peptide and substance P immunoreactivity in rat trigeminal ganglia and brainstem following adjuvant-induced inflammation of the temporomandibular joint. *Arch Oral Biol* 2000;45:335–345. [PubMed: 10708673]
44. Jensen L, Pilegaard H, Neufer PD, Hellsten Y. Effect of acute exercise and exercise training on VEGF splice variants in human skeletal muscle. *Am J Physiol Regul Integr Comp Physiol* 2004;287:R397–R402. [PubMed: 15117722]

45. Jones DA, Newham DJ, Round JM, Tolfree SE. Experimental human muscle damage: morphological changes in relation to other indices of damage. *J Physiol* 1986;375:435–448. [PubMed: 3025428]
46. Kano Y, Masuda K, Furukawa H, Sudo M, Mito K, Sakamoto K. Histological skeletal muscle damage and surface EMG relationships following eccentric contractions. *J Physiol Sci* 2008;58:349–355. [PubMed: 18838051]
47. Kano Y, Padilla DJ, Behnke BJ, Hageman KS, Musch TI, Poole DC. Effects of eccentric exercise on microcirculation and microvascular oxygen pressures in rat spinotrapezius muscle. *J Appl Physiol* 2005;99:1516–1522. [PubMed: 15994245]
48. Kantor TG. The pharmacological control of musculoskeletal pain. *Can J Physiol Pharmacol* 1991;69:713–718. [PubMed: 1863925]
49. Kehl LJ, Trempe TM, Hargreaves KM. A new animal model for assessing mechanisms and management of muscle hyperalgesia. *Pain* 2000;85:333–343. [PubMed: 10781907]
50. Kivela R, Silvennoinen M, Lehti M, Jalava S, Vihko V, Kainulainen H. Exercise-induced expression of angiogenic growth factors in skeletal muscle and in capillaries of healthy and diabetic mice. *Cardiovasc Diabetol* 2008;7:13. [PubMed: 18452614]
51. Kobayashi K, Fukuoka T, Obata K, Yamanaka H, Dai Y, Tokunaga A, Noguchi K. Distinct expression of TRPM8, TRPA1, and TRPV1 mRNAs in rat primary afferent neurons with delta/c-fibers and colocalization with trk receptors. *J Comp Neurol* 2005;493:596–606. [PubMed: 16304633]
52. Koh TJ, Brooks SV. Lengthening contractions are not required to induce protection from contraction-induced muscle injury. *Am J Physiol Regul Integr Comp Physiol* 2001;281:R155–R161. [PubMed: 11404289]
53. Liu A, Hoffman PW, Lu W, Bai G. NF-kappaB site interacts with Sp factors and up-regulates the NR1 promoter during neuronal differentiation. *J Biol Chem* 2004;279:17449–17458. [PubMed: 14970236]
54. Loram LC, Fuller A, Fick FG, Cartmell T, Poole S, Mitchell D. Cytokine Profiles During Carrageenan-Induced Inflammatory Hyperalgesia in Rat Muscle and Hind Paw. *J Pain* 2007;8:127–136. [PubMed: 16949880]
55. Lovering RM, De Deyne PG. Contractile function, sarcolemma integrity, and the loss of dystrophin after skeletal muscle eccentric contraction-induced injury. *Am J Physiol Cell Physiol* 2004;286:C230–C238. [PubMed: 14522817]
56. Lovering RM, Hakim M, Moorman CT III, De Deyne PG. The contribution of contractile pre-activation to loss of function after a single lengthening contraction. *J Biomech* 2005;38:1501–1507. [PubMed: 15922761]
57. Magni G, Caldieron C, Luchini SR, Merskey H. Chronic musculoskeletal pain and depressive symptoms in the general population. An analysis of the 1st National Health and Nutrition Examination Survey Data. *Pain* 1990;43:299–307. [PubMed: 2293141]
58. Malm C, Sjodin TL, Sjoberg B, Lenkei R, Renstrom P, Lundberg IE, Ekblom B. Leukocytes, cytokines, growth factors and hormones in human skeletal muscle and blood after uphill or downhill running. *J Physiol* 2004;556:983–1000. [PubMed: 14766942]
59. McLennan IS. Degenerating and regenerating skeletal muscles contain several subpopulations of macrophages with distinct spatial and temporal distributions. *J Anat* 1996;188:17–28. [PubMed: 8655404]
60. McLoughlin TJ, Mylona E, Hornberger TA, Esser KA, Pizza FX. Inflammatory cells in rat skeletal muscle are elevated after electrically stimulated contractions. *J Appl Physiol* 2003;94:876–882. [PubMed: 12433850]
61. McMahan SB, Sykova E, Wall PD, Woolf CJ, Gibson SJ. Neurogenic extravasation and substance P levels are low in muscle as compared to skin the rat hindlimb. *Neurosci Lett* 1984;52:235–240. [PubMed: 6084209]
62. McNeill C, Mohl ND, Rugh JD, Tanaka TT. Temporomandibular disorders: diagnosis, management, education, and research. *J Am Dent Assoc* 1990;120:253–263. [PubMed: 2179355]
63. Mense S. Sensitization of group IV muscle receptors to bradykinin by 5- hydroxytryptamine and prostaglandin E2. *Brain Res* 1981;225:95–105. [PubMed: 6271342]



64. Morgan DL, Gregory JE, Proske U. The influence of fatigue on damage from eccentric contractions in the gastrocnemius muscle of the cat. *J Physiol* 2004;561:841–850. [PubMed: 15486022]
65. Mueller, O.; Lightfoot, S.; Shroeder, A. RNA integrity number (RIN)- Standardization of RNA quality control. Waldbronn, Germany: Aligent Technologies; 2004.
66. Nahin RL, Byers MR. Adjuvant-induced inflammation of rat paw is associated with altered calcitonin gene-related peptide immunoreactivity within cell bodies and peripheral endings of primary afferent neurons. *J Comp Neurol* 1994;349:475–485. [PubMed: 7852637]
67. Nordstrom SH, Bishop M, Yemm R. The effect of jaw opening on the sarcomere length of the masseter and temporal muscles of the rat. *Arch Oral Biol* 1974;19:151–155. [PubMed: 4605242]
68. Nordstrom SH, Yemm R. Sarcomere length in the masseter muscle of the rat. *Arch Oral Biol* 1972;17:895–902. [PubMed: 4504651]
69. Norman RJ, Wu R. The potential danger of COX-2 inhibitors. *Fertil Steril* 2004;81:493–494. [PubMed: 15037388]
70. Ohlen A, Lindbom L, Staines W, Hokfelt T, Cuello AC, Fischer JA, Hedqvist P. Substance P and calcitonin gene-related peptide: immunohistochemical localisation and microvascular effects in rabbit skeletal muscle. *Naunyn Schmiedebergs Arch Pharmacol* 1987;336:87–93. [PubMed: 2442632]
71. Olesen J, Diener HC, Husstedt IW, Goadsby PJ, Hall D, Meier U, Pollentier S, Lesko LM. Calcitonin gene-related peptide receptor antagonist BIBN 4096 BS for the acute treatment of migraine. *N Engl J Med* 2004;350:1104–1110. [PubMed: 15014183]
72. Ono T, Maekawa K, Watanabe S, Oka H, Kuboki T. Muscle contraction accelerates IL-6 mRNA expression in the rat masseter muscle. *Arch Oral Biol* 2007;52:479–486. [PubMed: 17234151]
73. Pavlath GK, Thaloor D, Rando TA, Cheong M, English AW, Zheng B. Heterogeneity among muscle precursor cells in adult skeletal muscles with differing regenerative capacities. *Dev Dyn* 1998;212:495–508. [PubMed: 9707323]
74. Pedersen BK, Febbraio MA. Muscle as an endocrine organ: focus on muscle-derived interleukin-6. *Physiol Rev* 2008;88:1379–1406. [PubMed: 18923185]
75. Pizza FX, Peterson JM, Baas JH, Koh TJ. Neutrophils contribute to muscle injury and impair its resolution after lengthening contractions in mice. *J Physiol* 2005;562:899–913. [PubMed: 15550464]
76. Plesh, O.; Gansky, SA. Fibromyalgia. In: Laskin, DM.; Greene, CS.; Hylander, WL., editors. TMDs; An evidence-based approach to diagnosis and treatment. Chicago: Quintessence Publishing Co, Inc; 2006.
77. Plesh O, Wolfe F, Lane N. The relationship between fibromyalgia and temporomandibular disorders: Prevalence and symptom severity. *J Rheumatol* 1996;23:1948–1952. [PubMed: 8923373]
78. Radhakrishnan R, Moore SA, Sluka KA. Unilateral carrageenan injection into muscle or joint induces chronic bilateral hyperalgesia in rats. *Pain* 2003;104:567–577. [PubMed: 12927629]
79. Rayne J, Crawford GN. The relationship between fibre length, muscle excursion and jaw movements in the rat. *Arch Oral Biol* 1972;17:859–872. [PubMed: 4504647]
80. Reinert A, Kaske A, Mense S. Inflammation-induced increase in the density of neuropeptide-immunoreactive nerve endings in rat skeletal muscle. *Exp Brain Res* 1998;121:174–180. [PubMed: 9696386]
81. Reinohl J, Hoheisel U, Unger T, Mense S. Adenosine triphosphate as a stimulant for nociceptive and non-nociceptive muscle group IV receptors in the rat. *Neurosci Lett* 2003;338:25–28. [PubMed: 12565132]
82. Ren K. An improved method for assessing mechanical allodynia in the rat. *Physiol Behav* 1999;67:711–716. [PubMed: 10604842]
83. Ren K, Dubner R. Inflammatory Models of Pain and Hyperalgesia. *ILAR J* 1999;40:111–118. [PubMed: 11406689]
84. Rice TL, Chantler I, Loram LC. Neutralisation of muscle tumour necrosis factor alpha does not attenuate exercise-induced muscle pain but does improve muscle strength in healthy male volunteers. *Br J Sports Med* 2008;42:758–762. [PubMed: 17717057]

85. Richardson JD, Vasko MR. Cellular mechanisms of neurogenic inflammation. *J Pharmacol Exp Ther* 2002;302:839–845. [PubMed: 12183638]
86. Ro JY. Bite force measurement in awake rats: a behavioral model for persistent orofacial muscle pain and hyperalgesia. *J Orofac Pain* 2005;19:159–167. [PubMed: 15895839]
87. Ro JY, Capra NF. Modulation of jaw muscle spindle afferent activity following intramuscular injections with hypertonic saline. *Pain* 2001;92:117–127. [PubMed: 11323133]
88. Schafers M, Sorkin LS, Sommer C. Intramuscular injection of tumor necrosis factor- alpha induces muscle hyperalgesia in rats. *Pain* 2003;104:579–588. [PubMed: 12927630]
89. Shinoda M, Ozaki N, Sugiura Y. Involvement of ATP and its receptors on nociception in rat model of masseter muscle pain. *Pain* 2008;134:148–157. [PubMed: 17521813]
90. Smith LL, Brunetz MH, Chenier TC, McCammon MR, Houmard JA, Franklin ME, Israel RG. The effects of static and ballistic stretching on delayed onset muscle soreness and creatine kinase. *Res Q Exerc Sport* 1993;64:103–107. [PubMed: 8451526]
91. Sondell M, Lundborg G, Kanje M. Vascular endothelial growth factor has neurotrophic activity and stimulates axonal outgrowth, enhancing cell survival and Schwann cell proliferation in the peripheral nervous system. *J Neurosci* 1999;19:5731–5740. [PubMed: 10407014]
92. Steensberg A, Keller C, Starkie RL, Osada T, Febbraio MA, Pedersen BK. IL-6 and TNF-alpha expression in, and release from, contracting human skeletal muscle. *Am J Physiol Endocrinol Metab* 2002;283:E1272–E1278. [PubMed: 12388119]
93. Stewart LC, Deslauriers R, Kupriyanov VV. Relationships between cytosolic [ATP], [ATP]/[ADP] and ionic fluxes in the perfused rat heart: A <sup>31</sup>P, <sup>23</sup>Na and <sup>87</sup>Rb NMR study. *J Mol Cell Cardiol* 1994;26:1377–1392. [PubMed: 7869398]
94. Svensson P, Cairns BE, Wang K, Hu JW, Graven-Nielsen T, Arendt-Nielsen L, Sessle BJ. Glutamate-evoked pain and mechanical allodynia in the human masseter muscle. *Pain* 2003;101:221–227. [PubMed: 12583864]
95. Taguchi T, Matsuda T, Tamura R, Sato J, Mizumura K. Muscular mechanical hyperalgesia revealed by behavioural pain test and c-Fos expression in the spinal dorsal horn after eccentric contraction in rats. *J Physiol* 2005;564:259–268. [PubMed: 15677691]
96. Taguchi T, Sato J, Mizumura K. Augmented mechanical response of muscle thin-fiber sensory receptors recorded from rat muscle-nerve preparations in vitro after eccentric contraction. *J Neurophysiol* 2005;94:2822–2831. [PubMed: 16160095]
97. Takahashi K, Taguchi T, Itoh K, Okada K, Kawakita K, Mizumura K. Influence of surface anesthesia on the pressure pain threshold measured with different-sized probes. *Somatosens Mot Res* 2005;22:299–305. [PubMed: 16503582]
98. Tegeder L, Zimmermann J, Meller ST, Geisslinger G. Release of algescic substances in human experimental muscle pain. *Inflamm Res* 2002;51:393–402. [PubMed: 12234056]
99. Toda M, Suzuki T, Hosono K, Kurihara Y, Kurihara H, Hayashi I, Kitasato H, Hoka S, Majima M. Roles of calcitonin gene-related peptide in facilitation of wound healing and angiogenesis. *Biomed Pharmacother* 2008;62:352–359. [PubMed: 18430544]
100. Tsvitse SK, McLoughlin TJ, Peterson JM, Mylona E, McGregor SJ, Pizza FX. Downhill running in rats: influence on neutrophils, macrophages, and MyoD+ cells in skeletal muscle. *Eur J Appl Physiol* 2003;90:633–638. [PubMed: 12955516]
101. Uchiyama Y, Tamaki T, Fukuda H. Relationship between functional deficit and severity of experimental fast-strain injury of rat skeletal muscle. *Eur J Appl Physiol* 2001;85:1–9. [PubMed: 11513300]
102. Vijayan K, Thompson JL, Riley DA. Sarcomere lesion damage occurs mainly in slow fibers of reloaded rat adductor longus muscles. *J Appl Physiol* 1998;85:1017–1023. [PubMed: 9729578]
103. Watanabe M, Guo W, Zou S, Sugiyo S, Dubner R, Ren K. Antibody array analysis of peripheral and blood cytokine levels in rats after masseter inflammation. *Neurosci Lett* 2005;382:128–133. [PubMed: 15911135]
104. Weerakkody NS, Percival P, Hickey MW, Morgan DL, Gregory JE, Canny BJ, Proske U. Effects of local pressure and vibration on muscle pain from eccentric exercise and hypertonic saline. *Pain* 2003;105:425–435. [PubMed: 14527703]

105. Weijs WA. Mandibular movements of the albino rat during feeding. *J Morphol* 1975;145:107–124. [PubMed: 1111422]
106. Woolf C, Wiesenfeld-Halm Z. Substance P and calcitonin gene-related peptide synergistically modulate the gain of the nociceptive flexor withdrawal reflex in the rat. *Neurosci Lett* 1986;66:226–230. [PubMed: 2425287]

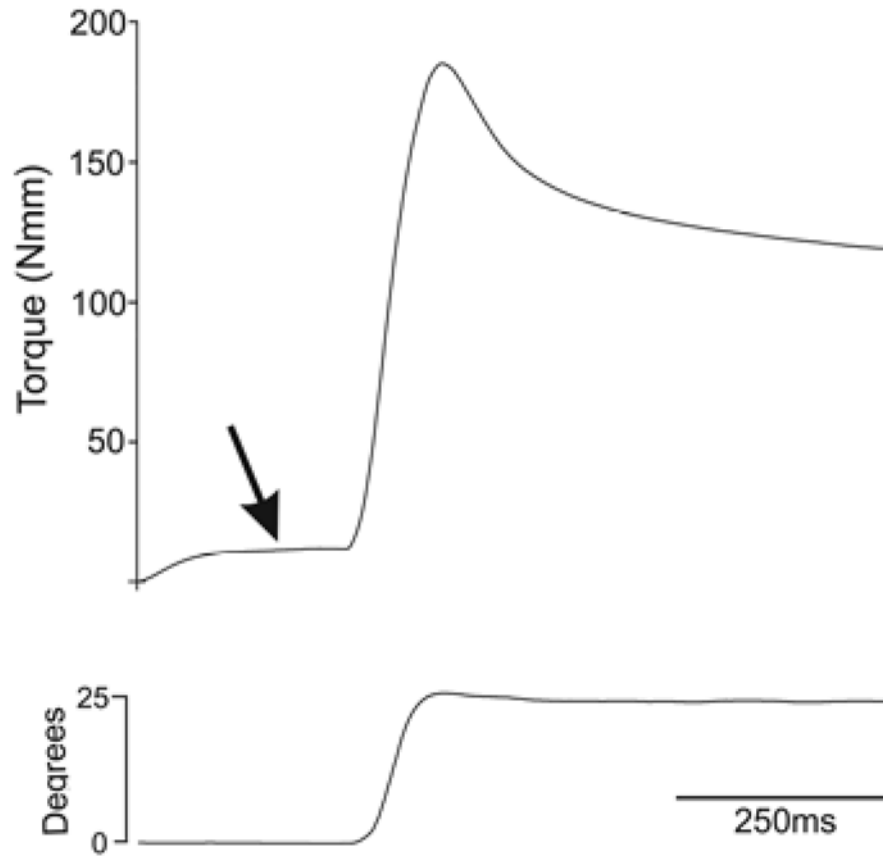


**Fig. 1.** Force and displacement during eccentric contraction of the masseter muscle. Upper trace shows typical torque developed during EC of the masseter muscle. Lower trace shows mandibular displacement during the EC. Note that the muscle is pre-activated (arrow) prior to muscle displacement (i.e. jaw opening).

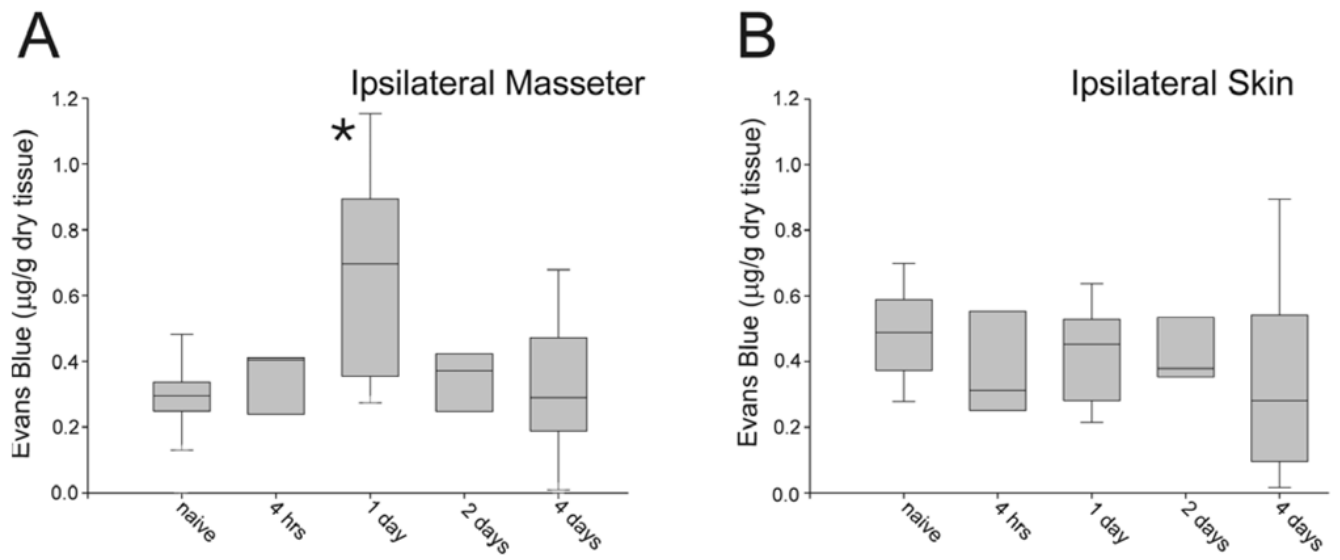


**Fig. 2.**

Plasma extravasation measured using Evans Blue after eccentric contraction of the masseter muscle. Note that significant plasma extravasation (asterisk,  $p < 0.05$ ) is evoked in the masseter 24h following EC but not in the overlying skin. Naive  $n = 26$ , 4h  $n = 7$ , 1d  $n = 13$ , 2d  $n = 6$ , 4d  $n = 12$ , Box plot shows median with edges of box denoting 25th and 75th percentile.

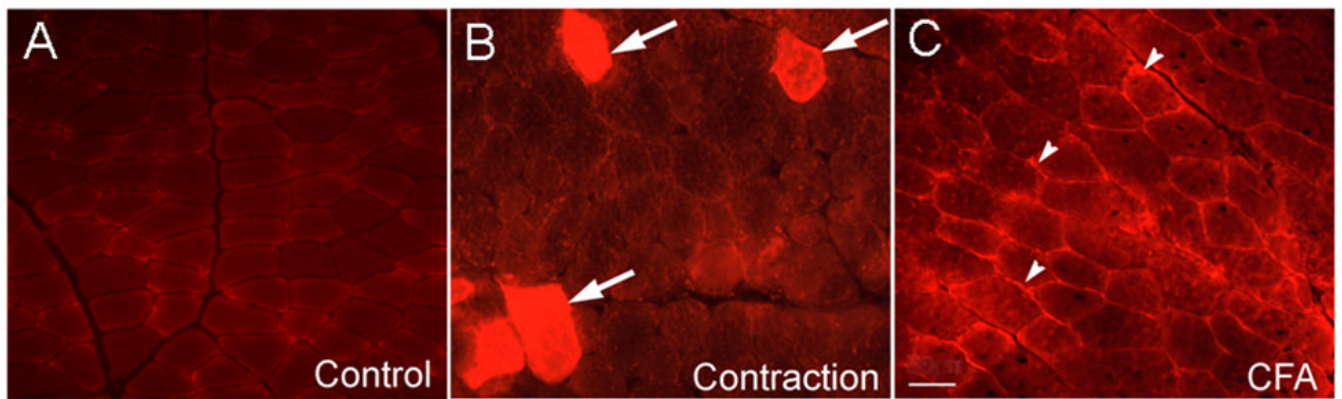


**Fig. 3.** Masseter muscle following systemic injection of Evans Blue. A: naive, B: 24h following EC, arrows point to myofibers containing Evans Blue indicative of membrane disruption. C: 24h following injection of CFA into masseter muscle. Arrowheads show the localization of Evans Blue in the extracellular space but not within myofibers. Scale bar=50 $\mu$ m

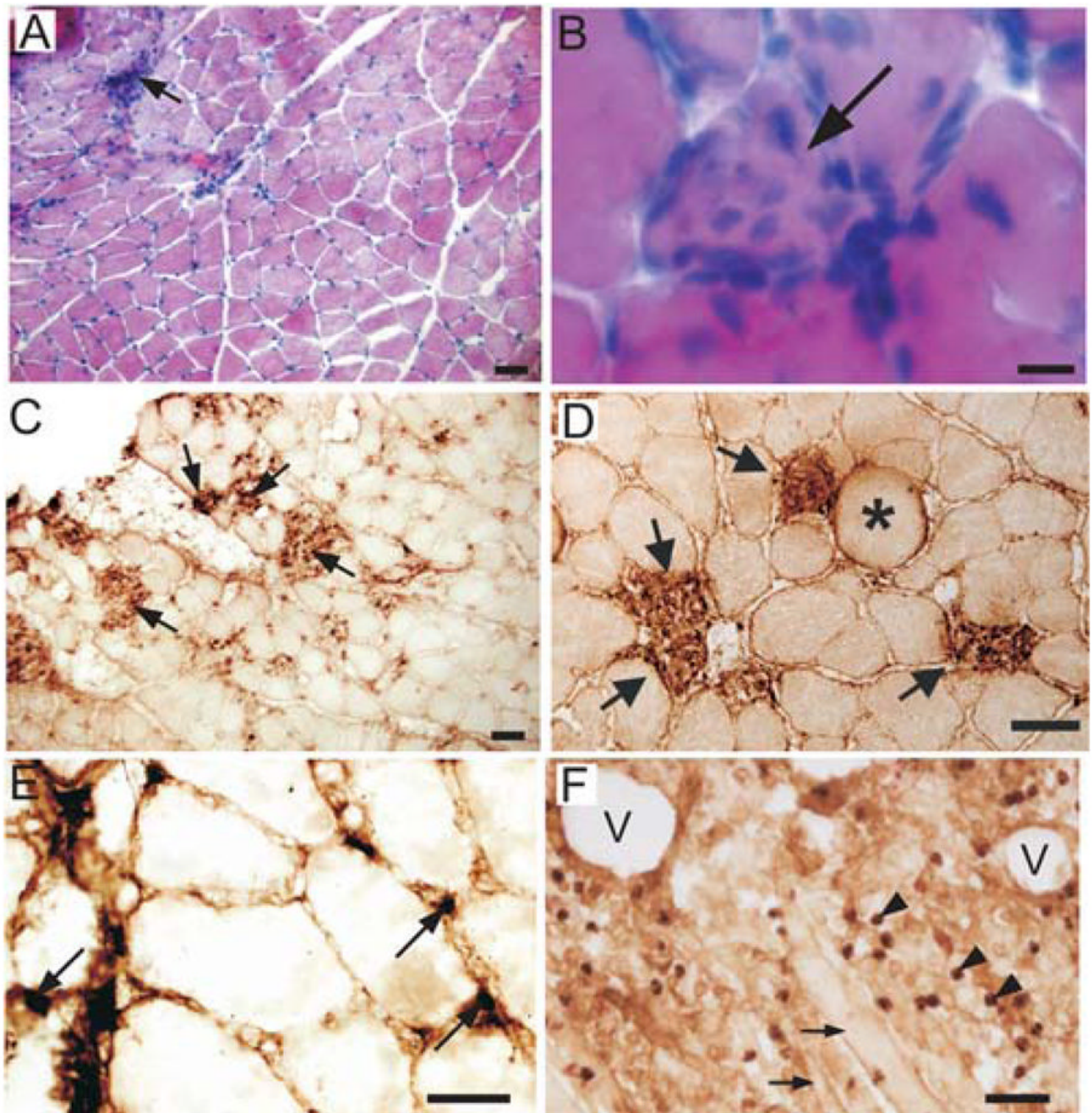


**Fig. 4.** Eccentric contraction evokes muscle inflammation with selective inflammatory cell infiltration of myofibers. A: H+E staining of the masseter muscle 48h after EC showing typical inflammatory cell infiltration (arrow). B: Higher magnification photomicrograph showing inflammatory cell infiltration into single masseter myofiber (arrow). C: Infiltration of masseter myofibers by ED1 macrophages (arrows) 96h after muscle contraction. D: Higher magnification photomicrograph showing selective infiltration of ED1 macrophages (arrows) into myofibers after EC. Asterisk denotes swollen myofiber. E: ED2 macrophages (arrows) in the masseter muscle 96h following contraction. F: Intramuscular injection of adjuvant produces massive non-specific inflammation with tissue erosion. Large vacuoles

(V) are evident, arrowheads identify ED1 macrophages, arrows point to myofibers. Scale bars A,C,D,F=50 $\mu$ m; B=10 $\mu$ m; E=25 $\mu$ m



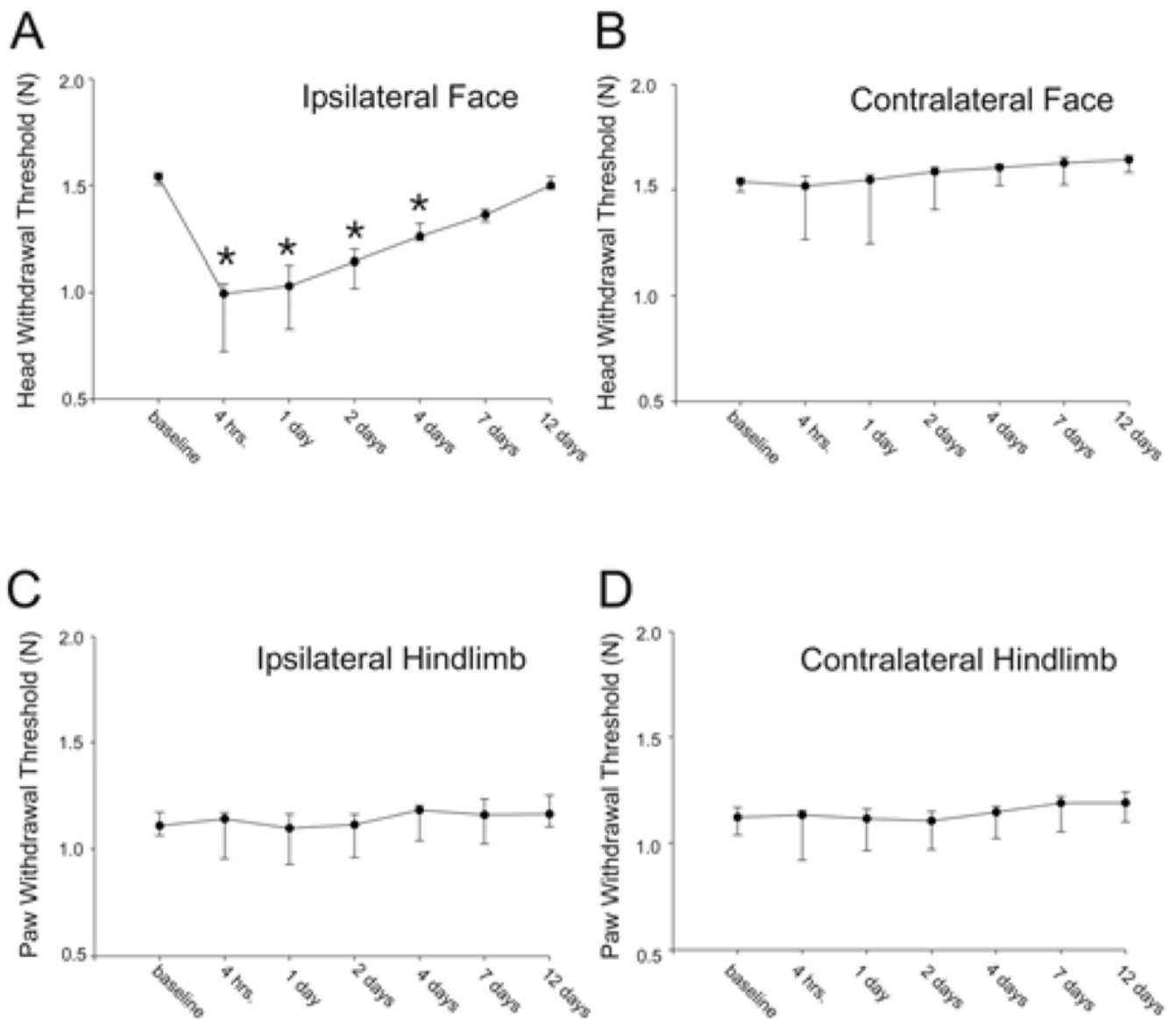


**Fig. 5.** Single bout of eccentric muscle contraction evoked ipsilateral mechanical hyperalgesia (asterisks denote significant reduction in head withdrawal threshold). Median values are plotted with the 25th and 75th percentile. Asterisks denote significant reduction in withdrawal threshold from baseline. n=10 animals

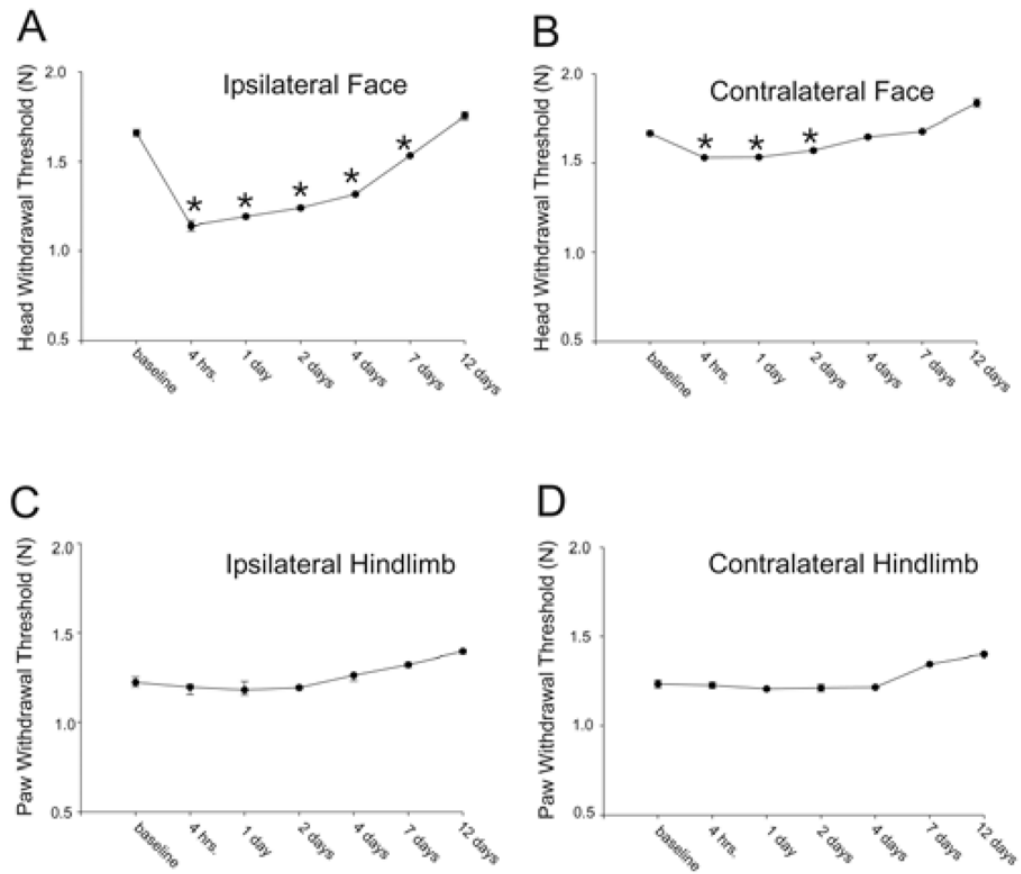


**Fig. 6.** Multiple bouts of eccentric contraction evokes ipsi- and bilateral mechanical hyperalgesia. Asterisks denote significant reduction in head withdrawal thresholds. Medians and 25th and 75th percentiles are plotted for comparison to Fig 5 even though parametric statistics were used for analysis. n=4 animals

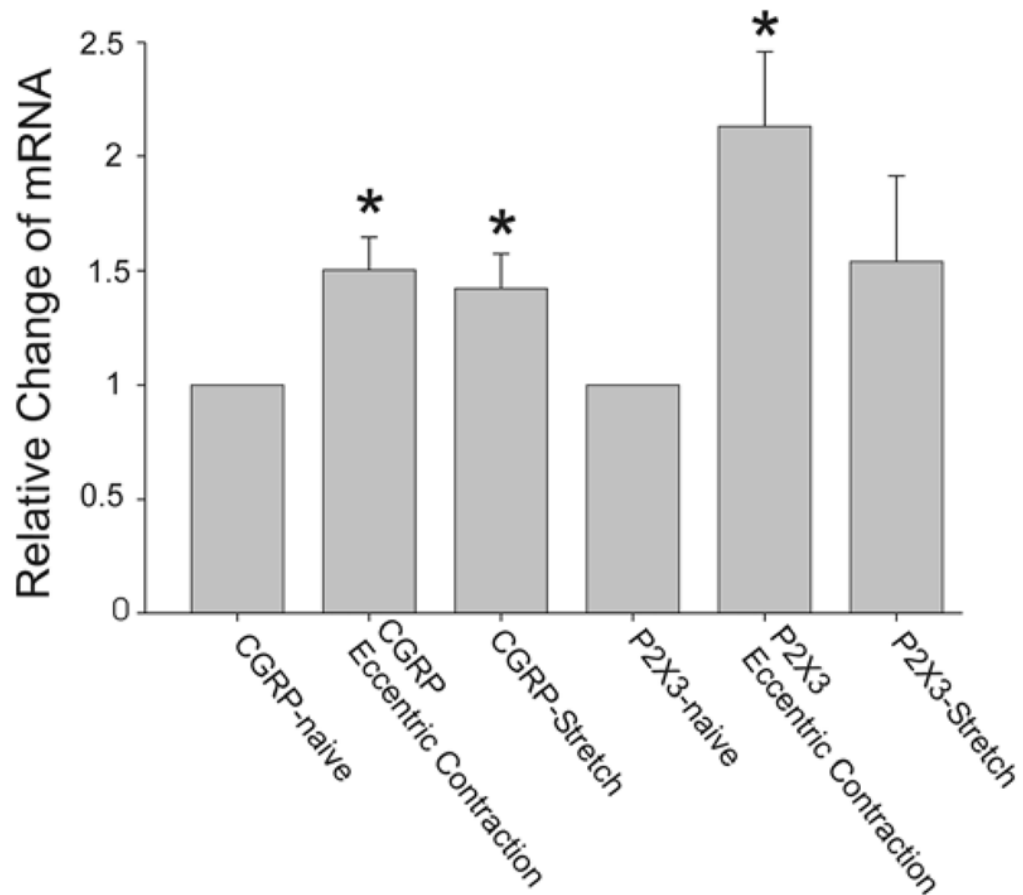


**Fig. 7.** Real-time polymerase chain reaction (RT-PCR) data from the ipsilateral mandibular division (V3) of the trigeminal ganglion 24h following eccentric muscle contraction. Means and SE are plotted, asterisks denote significant fold increases from naive. Note that both EC and rapid stretching increase CGRP mRNA while only EC increases P2X<sub>3</sub> mRNA at 24h.

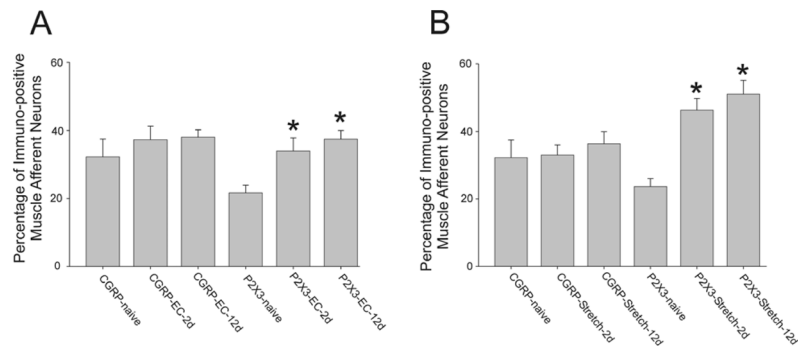


**Fig 8.** Percentage of immuno-positive muscle afferent neurons following eccentric muscle contraction and stretching. A. Percentage of CGRP and P2X<sub>3</sub> positive muscle afferent neurons following EC. Note the increase in P2X<sub>3</sub> muscle afferent neurons 2d and 12d following EC. B. Percentage of CGRP and P2X<sub>3</sub> muscle afferent neurons following stretching. Note the increase in P2X<sub>3</sub> muscle afferent neurons 2d and 12d following stretching. Means and SE are plotted, asterisks denote significant differences from naive.

**Table 1**

Masseter muscle edema.

	<b>n</b>	<b>mean</b> *	<b>SD</b>	<b>range</b> *
contracted	7	76.44	7.2	60.3 – 80.7
non-contracted	7	73.63	7.8	56.7 – 79.6

\*  
(wet weight – dry weight)/wet weight × 100